

Variations in the textural facies of sulphide minerals in the Eagle's Nest Ni-Cu-(PGE) deposit, McFaulds Lake greenstone belt, Superior Province, Ontario: Insights from microbeam scanning energy-dispersive X-ray fluorescence spectrometry

Natascia Zuccarelli¹, C. Michael Leshner¹, Michel G. Houlé², and Stephen J. Barnes³

¹Mineral Exploration Research Centre, Harquail School of Earth Sciences, Goodman School of Mines, Laurentian University, Sudbury, Ontario P3E 2C6

²Geological Survey of Canada, 490 rue de la Couronne, Québec, Quebec G1K 9A9

³Commonwealth Scientific and Industrial Research Organisation (CSIRO), Kensington, WA 6155, Australia

*Corresponding author's e-mail: nzuccarelli@pegoraro@laurentian.ca

ABSTRACT

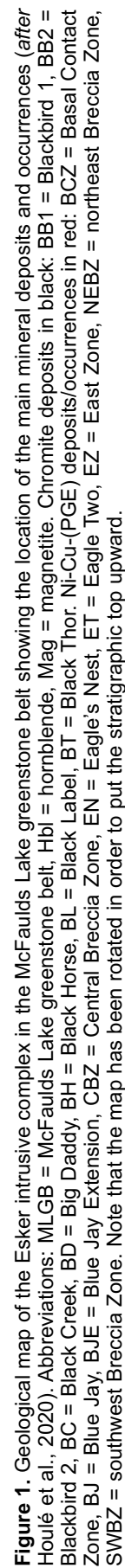
The Eagle's Nest Ni-Cu-(PGE) deposit occurs within the 2.73 Ga Esker intrusive complex of the Ring of Fire intrusive suite, in the McFaulds Lake greenstone belt of northern Ontario. Sulphide mineralization occurs along the northwestern margin of a subvertical ~500 m wide (north-south) \times \leq 85 m thick (east-west) \times >1500 m deep komatiitic ultramafic body composed of harzburgite \pm lherzolite \pm wehrlite that is interpreted to represent a structurally rotated, originally subhorizontal blade-shaped dyke. Disseminated (<15 wt% sulphide), net (15–35 wt% sulphide), and lesser semi-massive (50–80 wt% sulphide) and massive (>80 wt% sulphide) -textured sulphides have been characterized using microbeam scanning energy-dispersive X-ray fluorescence spectrometry (μ XRF). The images produced by this process have identified the abundances and locations of Fe, Ni, Cu, Ca, Si, and Cr within different minerals in 11 samples with representative sulphide textures: disseminated, leopard net-textured (containing bimodal coarse- and fine-grained olivine), pinto net-textured (containing bimodal coarse orthopyroxene and fine olivine), inclusion net-textured (containing coarse inclusions of peridotite), disrupted net-textured (containing pyroxenite invading leopard and pinto net-textured sulphides), semi-massive (containing inclusions of peridotite, pyroxenite, gabbro, and net-textured sulphides), and massive. All sulphide textures typically contain magmatic assemblages of pyrrhotite-pentlandite-chalcopyrite-magnetite \pm chromite. Notable differences include small ellipsoidal chromite inclusions only in facies with disseminated textures, little to no clinopyroxene in leopard net-textures, abundant clinopyroxene in invasive pyroxenite in disrupted net-textures, high-Cr orthopyroxene oikocrysts in pinto net-textures, and variable degrees of segregation of Cu-rich residual sulphide liquid from fractionally crystallizing Fe-Ni-rich monosulphide solid solution, more in disrupted and inclusion net-textures than in disseminated textures or leopard or pinto net-textures. The wide variety of net textures, the abundance of inclusions, and the invasive pyroxenite indicate a complex history for the magmatic plumbing system. Inclusions and late-stage pyroxenitic melt may have physically facilitated migration of residual sulphide liquid from monosulphide solid solution, and the emplacement of the late pyroxenite may have slowed cooling and/or reheated the mineralization. Many of these details are less evident visually in slabbed cores or polished thin sections, highlighting the usefulness of μ XRF in interpreting the genesis and beneficiation of texturally complex magmatic Ni-Cu-PGE ores.

INTRODUCTION

Most magmatic Ni-Cu-PGE ores form by the accumulation of an immiscible sulphide liquid that has scavenged chalcophile elements from a coexisting silicate liquid phase (*see* review by Naldrett, 2004). Most deposits contain multiple textural facies that reflect the mode(s) of emplacement of the sulphides (*see* review by Barnes et al., 2017). The Eagle's Nest Ni-Cu-(PGE) deposit in northern Ontario, contains a wide range of textures, some of which have previously not been

described, making it a particularly good site to evaluate the importance of ore textures in constraining ore genesis and beneficiation.

The Eagle's Nest deposit occurs within the 2.73 Ga Esker intrusive complex of the Ring of Fire intrusive suite within the McFaulds Lake greenstone belt of the north-central Superior Province in northern Ontario (Fig. 1, inset). The McFaulds Lake greenstone belt records episodic volcanism, sedimentation, ultramafic to felsic intrusive activity, and tectonism spanning



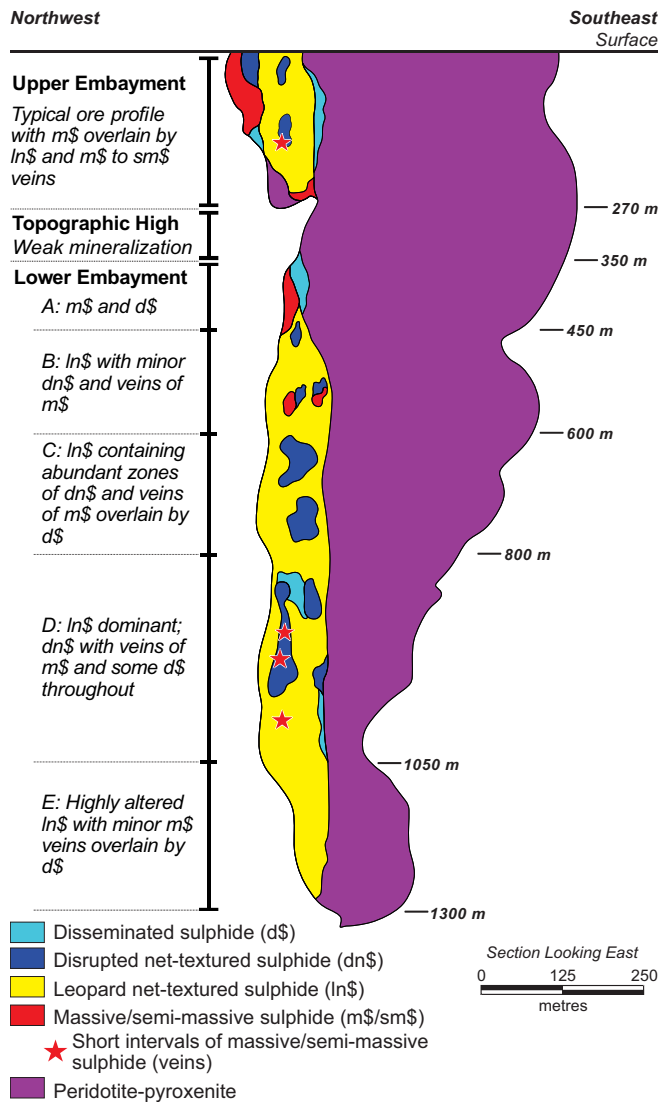


Figure 2. Schematic of a northwest-southeast section (NAD 83, Zone 16, UTM 547219 mE) through the Eagle's Nest dyke showing the sulphide facies and subfacies distributions. Note that the Eagle's Nest deposit occurs along the north-western contact with the country rocks. The location of the section is shown in Figure 1.

from at least 2.83 to 2.66 Ga (Metsaranta et al., 2015; Metsaranta and Houlé, 2020). This Archean basement is overlain by flat-lying Paleozoic carbonate-dominated strata and unconsolidated Quaternary deposits, making exploration challenging.

The Esker intrusive complex, which comprises the komatiitic Black Thor intrusion, Double Eagle intrusion, Eagle's Nest dyke, and many other intrusive bodies (Fig. 1), represents an ultramafic-dominated intrusive complex that experienced high magma flux through and crystallization/accumulation within originally smaller, dynamic, komatiitic intrusions/conduits that are interpreted to have coalesced laterally over time through magma inflation to form the present 16 km long Cr- and Ni-Cu-(PGE) mineralized complex

(Houlé et al., 2019, 2020). The Eagle's Nest intrusion is a subvertical ~ 500 m wide (north-south) \times ~ 85 m thick (east-west) \times >1500 m deep body composed of harzburgite \pm lherzolite \pm wehrlite within tonalitic country rocks, with the deposit occurring along the north-western margin of the dyke (Fig. 2). It is interpreted to have been emplaced as a subhorizontal blade-shaped dyke (Barnes and Mungall, 2018; Zuccarelli et al., 2018a) and to have been structurally rotated (along with the rest of the Esker intrusive complex) into its current subvertical orientation (Mungall et al., 2010; Zuccarelli et al., 2018a,b; Laudadio, 2019). All of the rocks have been metamorphosed to greenschist facies and are locally deformed, but the stress was partitioned into discrete shear zones (e.g. Frank Shear Zone: Laudadio, 2019) so most of the ores and host rocks are not penetratively deformed and exhibit well preserved igneous textures.

The purpose of this contribution is to report the results of microbeam scanning energy-dispersive X-ray fluorescence spectrometry (μ XRF) mapping of the representative textural sulphide facies at the Eagle's Nest Ni-Cu-(PGE) deposit to not only supplement the petrographic work undertaken by Zuccarelli (M.Sc. in prep) but also to provide insights on the mechanisms involved in the formation of textural sulphide facies within magmatic Ni-Cu-(PGE) deposits.

METHODS

During this M.Sc. project, the surfaces of two hundred representative samples of half NQ (47.6 mm diameter) core were ground on a diamond-bonded lap and examined mesoscopically using a stereomicroscope. Thin sections were prepared of representative parts of the cores and examined microscopically in reflected and transmitted light using a compound polarizing microscope. The mineralogical and textural information collected about these samples was used to guide textural classification and the selection of a subset of 11 samples (1 patchy/blebby disseminated, 3 leopard net-textured, 2 pinto net-textured, 1 inclusion net-textured, 2 disrupted net-textured, 1 semi-massive, and 1 massive sulphide) for chemical/mineralogical characterization using a Bruker TornadoTM high-resolution desktop μ XRF at the Commonwealth Scientific and Industrial Research Organisation (CSIRO) in Perth (Western Australia). Analyses utilized a ~ 40 micron diameter collimated X-ray beam generated from an Rh target tube operating at 50 kV and 500 nA without filters and an XFlash VR silicon drift detector. The sample was rastered under the beam with dwell times typically 5 to 10 ms per pixel, at a spatial resolution of 40 microns. Each map is presented as a composite red-green-blue (RGB) image showing the distributions of combinations of three elements (Cr-Fe-Ca, Ni-Cu-S, and S-Fe-

Table 1. Principal characteristics of sulphide textural facies and subfacies in magmatic Ni-Cu-PGE deposits at the Eagle's Nest Ni-Cu-(PGE) deposit.

Sulphide Textural Facies	Nominal Sulphide Content (wt%)	Nominal Sulphur Content (wt%)	Eagle's Nest Deposit			
			Sulphide Content (wt%)	Proportion (%)	Thickness (m)	Strike Length ¹ (m)
Disseminated*	<15	<5.9	<15	5		
Lightly**	<5	<2.0	0.5–5	14		
Medium**	5–10	2.0–3.9	5–10	42	up to 20	up to 125
Heavily**	10–15	4.0–5.9	10–15	21		
Patchy**	<15	<5.9	8–10	9		
Blebbly**	<15	<5.9	2–5	14		
Net-Textured*	15–60	5.9–23.4	15–35	80		
Leopard**			15–35	52		
Patchy**			15–25	14	up to 40	up to 130
Inclusion**			15–30	5		
Pinto**			15–30	1		
Disrupted**			18–25	28		
Semi-Massive*	50–80	19.5–31.2	50–80	15	up to 20	up to 40
Massive*	>80	>31.2	>80			

*Based on Noront Resources Ltd. assay data set that contains more than 10,000 assays and assuming 39 wt% S in 100% sulphide; **based on 200 representative samples examined in this study. Sulphide textural facies and sub-facies are generally gradational with some overlap of sulphide or sulphur contents, particularly in samples containing 50–60% sulphide. Thickness and strike length have been estimated based on a detailed geological map from Noront Resources Ltd. ¹Corresponds to the ore surface projection of each textural sulphide facies.

Ca) at various scales. Minerals containing none of the elements appear black, minerals containing one of the three elements appear in the corresponding colour, minerals containing equal amounts of two or three of the elements appear in composite colours (e.g. 1 green + 1 blue = cyan, 1 red + 1 green = yellow, 1 red + 1 blue = magenta, 1 red + 1 green + 1 blue = white), and minerals containing unequal amounts of two or three of the elements appear in intermediate colours (e.g. 2 red + 1 green = orange). Each channel is normalized to the minimum and maximum count rate per pixel over the entire map; hence, where concentrations of a particular element are low, this normalization process will exaggerate backgrounds and can produce artifacts. Diffraction artefacts can also occur at low element concentrations, arising from geometry, whereby a particular crystal is aligned with a lattice plane making a Bragg angle with the input beam and the detector, although these are usually only evident in unaltered well crystalline rocks.

SULPHIDE TEXTURAL FACIES

The Eagle's Nest Ni-Cu-(PGE) deposit contains a wide range of sulphide textural facies: 1) disseminated, 2) net-textured, 3) semi-massive, and 4) massive sulphides (Table 1). The ore assemblage in all facies is a typical magmatic assemblage of pyrrhotite >> pentlandite > chalcopyrite >> magnetite±chromite. There is a general upward trend of the ore profile from discontinuous massive sulphide through more continuous net-

textured to disseminated sulphide (Fig. 2). The contacts between the zones are generally relatively sharp; however, the contacts between the various net-textured facies vary from sharp to gradational. Most net-textured subfacies vary non-systematically on scales of 10 to 20 m, whereas disrupted net-textured sulphides vary on a scale of 2 to 10 cm.

Many crosscutting relationships and inclusions occur between and within the sulphide facies at Eagle's Nest (Mungall et al., 2010; Zuccarelli et al., 2017; Zuccarelli, in prep). Although the majority of massive sulphides are localized in shallow footwall embayments, massive sulphides veins (1–100 cm thick) containing inclusions of leopard and disrupted net-textured facies and barren gabbroic rocks crosscut disseminated and net-textured facies. Disrupted net-textured facies contain inclusions of net-textured olivine-sulphide cumulates, inclusion net-textured sulphides contain inclusions of barren peridotite, and disseminated sulphide facies contain inclusions of massive chromitite.

Disseminated Sulphide Facies

Disseminated sulphide facies generally contains <15 wt% sulphide and ≤6 wt% S. Mineralization is distributed heterogeneously across the deposit, most commonly between underlying net-textured sulphides and overlying barren host rocks. Disseminated sulphides occur as lightly, medium, heavily, patchy, and blebby disseminated subfacies. Lightly disseminated sulphide

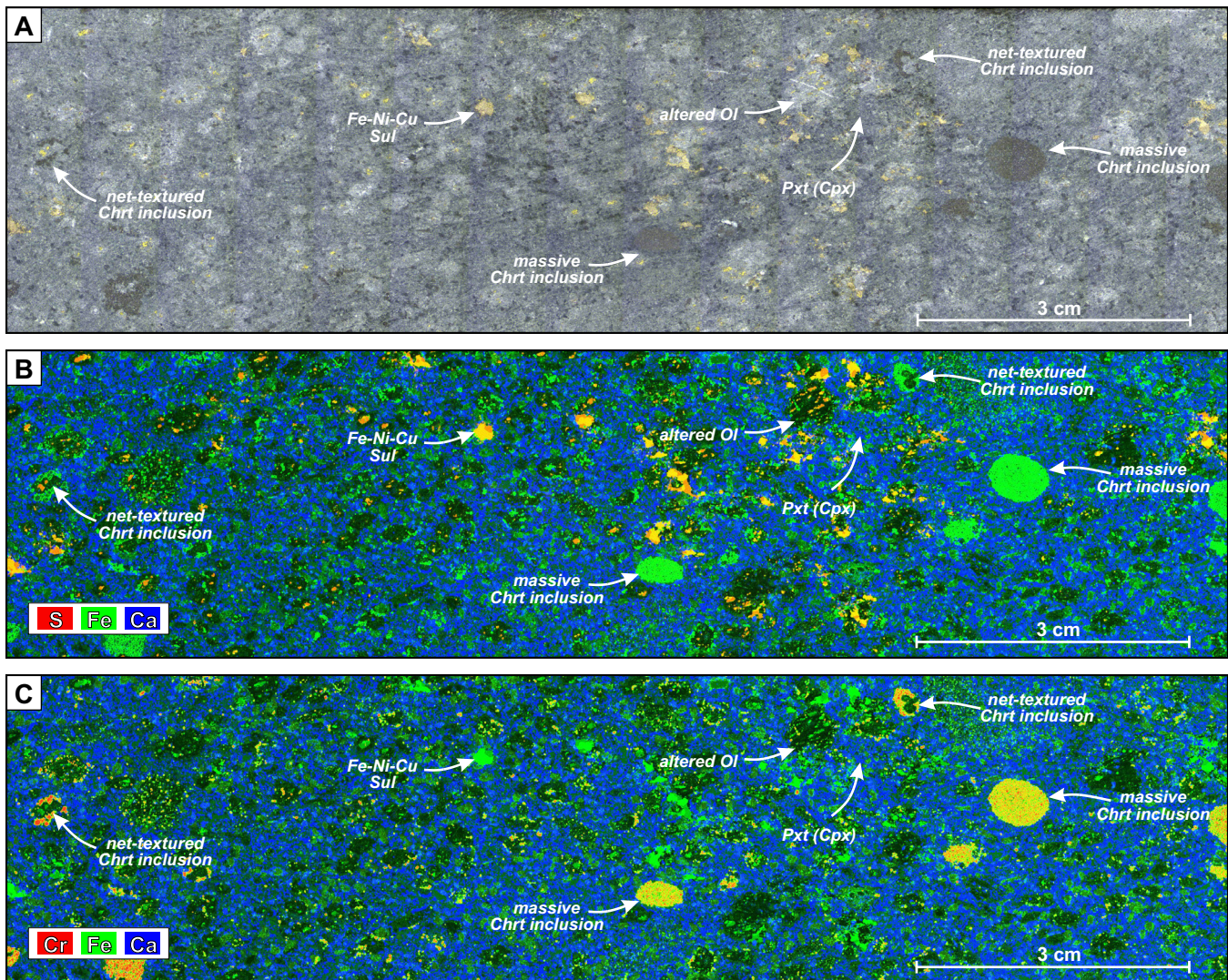


Figure 3. Disseminated sulphide facies at the Eagle's Nest deposit (drill core NOT-09-053W3 at 828.17 m, NQ core size). **a)** A scanned slab showing the typical disseminated sulphide texture within olivine pyroxenite. Black phases are chromite, dark grey phases are olivine, grey phases are pyroxene, and yellowish phases are sulphide. **b)** μ XRF map, normalized relative concentrations of Ca (blue), Fe (green), and S (red). **c)** μ XRF map, normalized relative concentrations of Cr (red), Fe (green), and Ca (blue). Chromite-magnetite aggregates in orange. Abbreviations: Chrt = chromitite, Cpx = clinopyroxene, Ol = olivine, Pxt = pyroxenite, Sul = sulphides.

occurs as 0.5–5 wt% sulphide distributed in very fine (0.2–0.5 mm) grains. Medium disseminated sulphide occurs as 5–10% sulphide in small to medium (0.5–10 mm) irregular wisps. Heavily disseminated sulphide occurs as 10–15 wt% sulphide in 10–30 mm irregular wisps. Patchy disseminated sulphide (8–10 wt% sulphide) occurs as very small to small (<0.5–40 mm), isolated, unevenly to uniformly dispersed, irregular patches. Blebbly disseminated sulphide (2–5 wt% sulphide) occurs as small to medium (20–40 mm), rounded to subrounded blebs in the interstitial spaces between olivine and pyroxene in peridotite and pyroxenite. The sulphides within coarser blebs are occasionally fractionated with chalcopyrite-rich upperparts and pyrrhotite-pentlandite-rich lower parts, whereas finer blebs are rarely systematically fractionated.

A typical example of 8 wt% patchy disseminated sulphides within an olivine pyroxenite is shown in Figure 3 (optical scan in Fig. 3a and μ XRF maps in Fig. 3b,c). The optical scan shows that sulphide is concentrated in domains containing abundant dark serpentinized olivine crystals and that several ellipsoidal chromitite inclusions are also present. However, these observations are much clearer in the μ XRF maps. In the S-Fe-Ca map (Fig. 3b), it is obvious that sulphide phases (yellow and orange colours) are more abundant in olivine-rich domains (dark green), that there are few sulphides in clinopyroxene- (blue) and orthopyroxene- (green) rich domains, and that clinopyroxene-rich domains contain ellipsoidal peridotite (dark and medium green) and chromitite (bright green) inclusions. Some of the latter are embayed. In the Cr-Fe-Ca

map (Fig. 3c), it is possible to identify two types of chromitite inclusions: 1) net-textured chromitite, where chromite occurs as clusters of single crystals (red to yellow) within olivine-rich domains (dark to dark green) and 2) ellipsoidal massive chromitite inclusions exhibiting varying degrees of alteration to ferrichromite (i.e. red = Cr-rich core, yellow = Cr-poor rim). These textures are more complex than the more uniformly disseminated sulphides in most Ni-Cu-PGE deposits (see Barnes et al., 2017).

Net-Textured Sulphide Facies

Net-textured sulphide facies typically contains ~15–35 wt% sulphide and ~6–14 wt% S and occurs along the entire length of the deposit. It consists of ~65–85% mesocumulus olivine with ~15–35 wt% sulphides that form thin films between the olivine. However, these facies exhibit wide textural variations in the Eagle's Nest deposit, which can be subdivided into five subfacies that differ in their distribution of sulphide and silicate minerals.

Leopard net-textured sulphide subfacies

Leopard net-textured sulphide subfacies is the most common net-textured subfacies at Eagle's Nest. It consists of ~65–85% cumulus olivine and lesser intercumulus pyroxene with ~15–35 wt% interstitial sulphide that forms thin films between the olivine and triangular-shaped patches between olivine±pyroxene. Olivine and pyroxene are bimodal, ranging in size from 1–3 mm and 5–15 mm. The coarser crystals and lesser crystal aggregates define this as “leopard net-textured” because the large pseudomorphs of serpentine-magnetite after olivine appear as black spots among the network of yellowish sulphides giving the appearance of a leopard's coat. The sulphide assemblage is composed of pyrrhotite > pentlandite > chalcopyrite.

A typical example of the leopard net-textured sulphide subfacies rock is shown in Figure 4 (optical scan in Fig. 4a and μ XRF maps in Fig. 4b,c). In the optical image (Fig. 4a), the sulphides are evenly distributed except within serpentinized olivine mesocrysts (dark black) and fine-grained aggregates (dark-greyish black phases). In the Ni-Cu-S map (Fig. 4b), abundant chalcopyrite (green) forms an anastomosing network around very fine and very coarse olivine (black), most of the pentlandite (magenta) occurs more sporadically, and most of the pyrrhotite (blue) defines a foliation oriented at ~60° to the core axis and ~60° to a weak igneous lamination defined by the olivine aggregates. This particular hole was drilled subparallel to the basal contact of the intrusion and the orientation of the sawn surface was not necessarily perpendicular to the foliation and as a result, the sulphide foliation may be a bit more perpendicular but the igneous lamination cannot

be any less oblique. In the Cr-Fe-Ca map (Fig. 4c), coarse serpentinized olivine (black) is oikocrystic, containing fine chromite (red) and ferrichromite (yellow) chadacrysts, or is xenolithic comprising inclusions of chromite-bearing dunite. The matrix consists of fine disseminated clinopyroxene (blue) and Fe-bearing sulphides (green).

Pinto net-textured sulphide subfacies

Pinto net-textured sulphide subfacies, which is characterized by white (talc-altered orthopyroxene) rather than grey (clinopyroxene) or black (serpentinized olivine) “spots”, is uncommon at Eagle's Nest. It comprises ~15–30 wt% sulphides and ~6–12 wt% S and most commonly occurs as 1–2 m zones within areas of disrupted net-textured sulphides and where domains of leopard net-textured sulphide facies rocks border pyroxene-rich domains. It is texturally similar to leopard net-textured subfacies rock and consists of small serpentinized olivine surrounded by interstitial sulphides with large (0.3–10 mm) subhedral-euhedral oikocrysts of talc-carbonate-altered orthopyroxene (appearing whitish-grey in the core). The oikocrysts contain both fresh and serpentinized olivine.

A typical example of pinto net-textured sulphide subfacies rock is shown in Figure 5 (optical scan in Fig. 5a, μ XRF maps in Fig. 5b,c). In the optical image (Fig. 5a) the amount of sulphide is relatively small (~20–25%) and occurs almost exclusively in close association with small serpentinized olivine crystals (black) that are interstitial to coarse sulphide-free orthopyroxene oikocrysts (grey). In the Ni-Cu-S map (Fig. 5b), pyrrhotite (blue), pentlandite (magenta), and chalcopyrite (green) are more-or-less evenly disseminated throughout the sample except within the large weakly aligned pyroxene domains (black). Nevertheless, chalcopyrite is more common on the peripheries of the pyroxene oikocrysts. In the Cr-Fe-Ca map (Fig. 5c), the matrix is dominated by sulphides (green) and fine-grained olivine (greenish-black), and the pyroxene-rich domains include parts comprising mainly orthopyroxene (reddish-brown), chromite (red), and ferrichromite (orange and yellow) as well as parts comprising mainly clinopyroxene (blue).

Inclusion net-textured sulphide subfacies

Inclusion net-texture sulphide subfacies, which is another uncommon variety of net-textured sulphide at Eagle's Nest, contains ~15–30 wt% sulphide and ~6–12 wt% S. It is similar to the leopard net-textured sulphide subfacies except that it contains a greater abundance of clinopyroxene (~10–15% silicates) and is characterized by 4–300 mm silicate inclusions. The inclusions are typically dunite to peridotite, vary in shape from angular to rounded, and the contacts

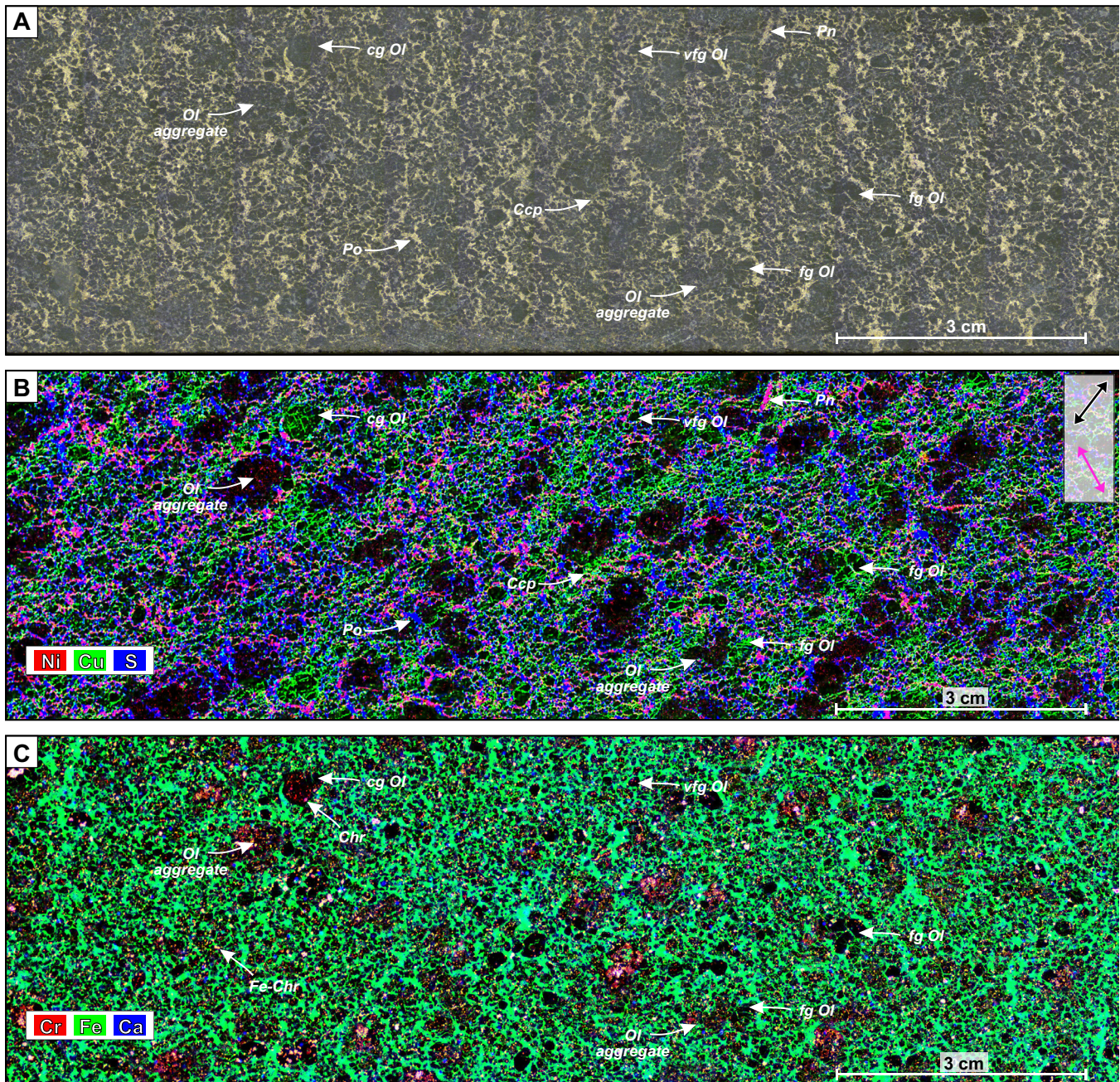


Figure 4. Leopard net-textured sulphide subfacies at Eagle's Nest deposit (drill core NOT-07-017 at 138.01 m, NQ core size). **a)** A scanned slab of a typical leopard net-textured sulphide. The black minerals are serpentinized olivine and the yellowish minerals are sulphide minerals including pyrrhotite, pentlandite, and chalcopyrite. However, these sulphide minerals are difficult to distinguish. **b)** μ XRF map with normalized relative concentrations of Ni (red), Cu (green), and S (blue) resulting in olivine appearing as black, chalcopyrite as green, pyrrhotite as blue, and pentlandite as magenta. **c)** μ XRF map with normalized relative concentrations of Cr (red), Fe (green), and Ca (blue) resulting in olivine appearing as black, chromite as red, ferrichromite as yellow, clinopyroxene as blue and Fe-bearing sulphides as green. The black arrow indicates the direction of a weak igneous lamination defined by the alignment of the olivine aggregates; the magenta arrow indicates the direction of the weak foliation defined by pentlandite±pyrrhotite veinlets. Abbreviations: cg = coarse-grained, fg = fine-grained, vfg = very fine-grained; Ccp = chalcopyrite, Chr = chromite, Fe-Chr = ferrichromite, Ol = olivine, Pn = pentlandite, Po = pyrrhotite.

between olivine and pyroxene along the margins are diffuse and infiltrated by sulphide (typically chalcopyrite). One particularly large (30 cm) inclusion is exceptionally angular but also exhibits irregular and diffuse margins (Zuccarelli, in prep).

A typical example of inclusion net-textured sulphide

subfacies rock containing ~25 wt% sulphides is shown in Figure 6. In the optical image (Fig. 6a), sulphide is not evenly distributed and is controlled mainly by the distribution of inclusions and, to a lesser extent, olivine. The three main domains can be defined: 1) chalcopyrite-pentlandite-(pyrrhotite), 2) pentlandite-pyrrhotite-

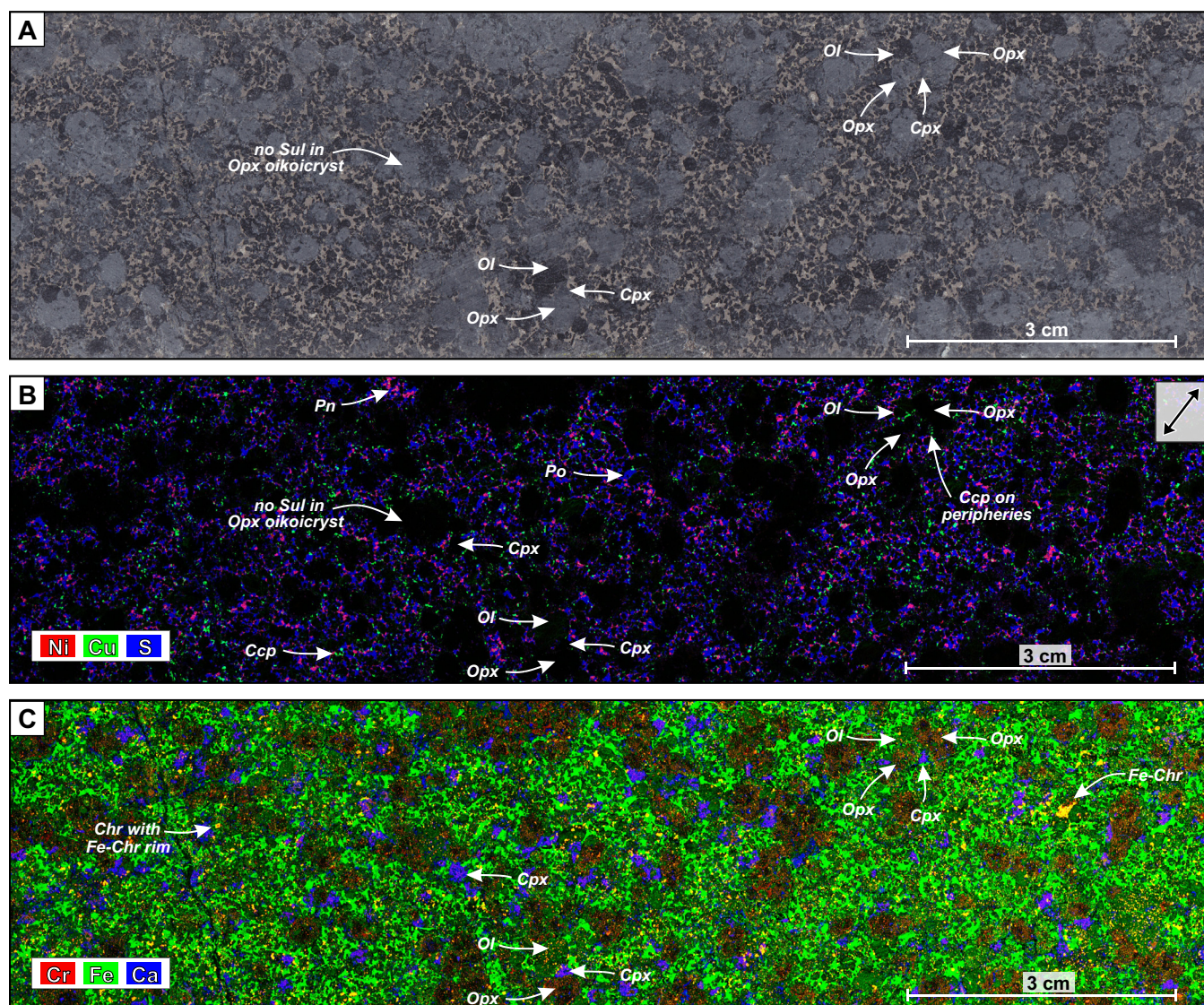


Figure 5. Pinto net-textured sulphide subfacies at the Eagle's Nest deposit (sample NOT-10-076-W1/557.1 m, NQ core size). **a)** A scanned slab of typical pinto net-textured sulphide. The black minerals are olivine, grey minerals are pyroxene, and yellowish minerals are sulphide. **b)** μ XRF map with normalized relative concentrations of Ni (red), Cu (green), and S (blue) with pyrrhotite appearing as blue, pentlandite as magenta, and chalcopyrite as green. **c)** μ XRF map with normalized relative concentrations of Cr (red), Fe (green), and Ca (blue) resulting in the sulphides appearing as green, olivine as greenish-black, orthopyroxene-rich domains as reddish-brown, chromite as red, ferrichromite as yellow and orange, and clinopyroxene as blue. The black arrow indicates the direction of the weak lamination defined by orthopyroxene oikocrysts. Abbreviations: Ccp = chalcopyrite, Cpx = clinopyroxene, Chr = chromite, Fe-Chr = ferrichromite, Ol = olivine, Opx = orthopyroxene, Pn = pentlandite, Po = pyrrhotite, Sul = sulphides.

(chalcopyrite), and 3) chalcopyrite-pyrrhotite-pentlandite. In the Ni-Cu-S map (Fig. 6b), pentlandite (magenta), pyrrhotite (blue), and lesser chalcopyrite (cyan or green) occur both in large domains with silicates (reddish-black in this image) and in fine pyrrhotite-pentlandite-rich veinlets oriented at $\sim 90^\circ$ to the core axis (subparallel to the dyke contact). Chalcopyrite, silicates, and lesser pyrrhotite-pentlandite dominate the other domains. In the Cr-Fe-Ca map (Fig. 6c), it is clear that the silicate phases include coarse-grained olivine (black) containing small inclusions of chromite (red), orthopyroxene (opalescent), medium-grained clinopyroxene (blue), and fine-grained olivine

(black) within sulphide (green). The 1 cm dunite auto-lith in this sample is a serpentinized peridotite composed of serpentine (black) with magnetite (green) veinlets and fine chromite inclusions (red).

Disrupted net-textured sulphide subfacies

Disrupted net-textured sulphide subfacies is a localized but common form of net texture in Eagle's Nest, containing ~ 18 – 25 wt% sulphide and ~ 7 – 10 wt% S. It is characterized by highly irregular domains of grey talc-magnesite-altered pyroxenite that transgresses leopard net-texture and consists of coarse (up to 4 mm) serpentinized olivine in a matrix of fine serpentinized olivine

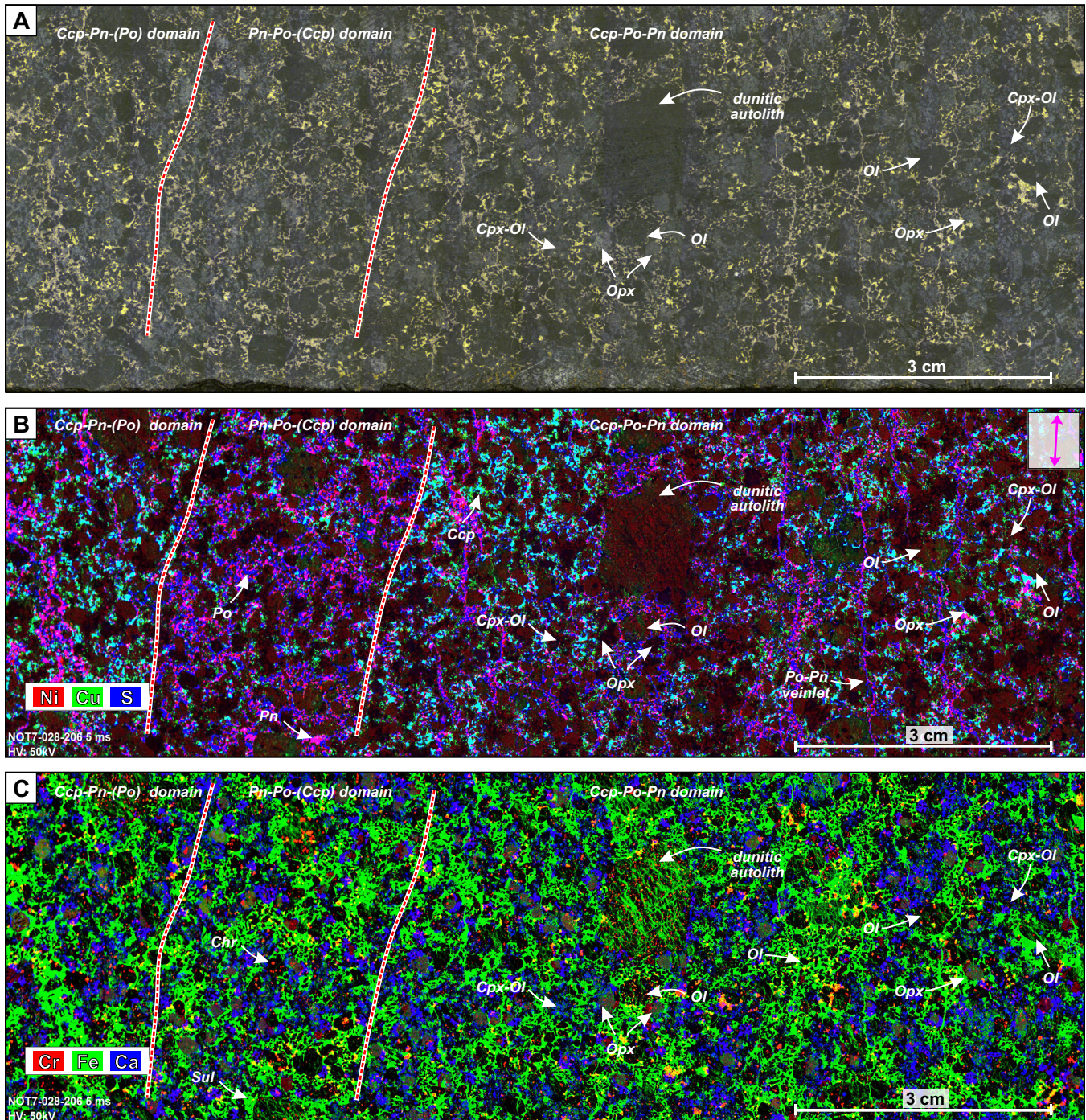


Figure 6. Inclusion net-textured sulphide subfacies at the Eagle's Nest deposit (drill core NOT-07-028 at 208.97 m, NQ core size). **a)** A scanned slab of a typical inclusion net-textured sulphide facies rock from the Eagle's Nest deposit. The black minerals are olivine and the yellowish minerals are sulphide. **b)** μ XRF map with normalized relative concentrations of Ni (red), Cu (green), and S (blue). **c)** μ XRF map with normalized relative concentrations of Cr (red), Fe (green), and Ca (blue). Red-dashed lines show the approximate limit between pentlandite-pyrrhotite-rich and chalcopyrite-rich domains; the magenta arrow in (b) indicates the orientation of the fine veinlets of pentlandite and pyrrhotite. Abbreviations: Ccp = chalcopyrite, Chr = chromite, Cpx = clinopyroxene, Ol = olivine, Opx = orthopyroxene, Pn = pentlandite, Po = pyrrhotite.

and sulphides, often leaving isolated coarse unserpentinized olivine but not any fine-grained olivine or sulphides. The contacts between the pyroxenite domains and net-textured sulphides are very irregular. The most abundant sulphide mineral in this subfacies is pyrrhotite, with varying amounts of fine-grained pentlandite (0.1–

0.5 mm) and chalcopyrite (0.1–3 mm). Magnetite occurs in both barren and mineralized areas, forming grains of up to 0.5 mm in apparent diameter that range from anhedral to euhedral. Minor chromite is also present.

A typical example of disrupted net-textured sulphide subfacies rock, containing ~25 wt% sulphides, is shown

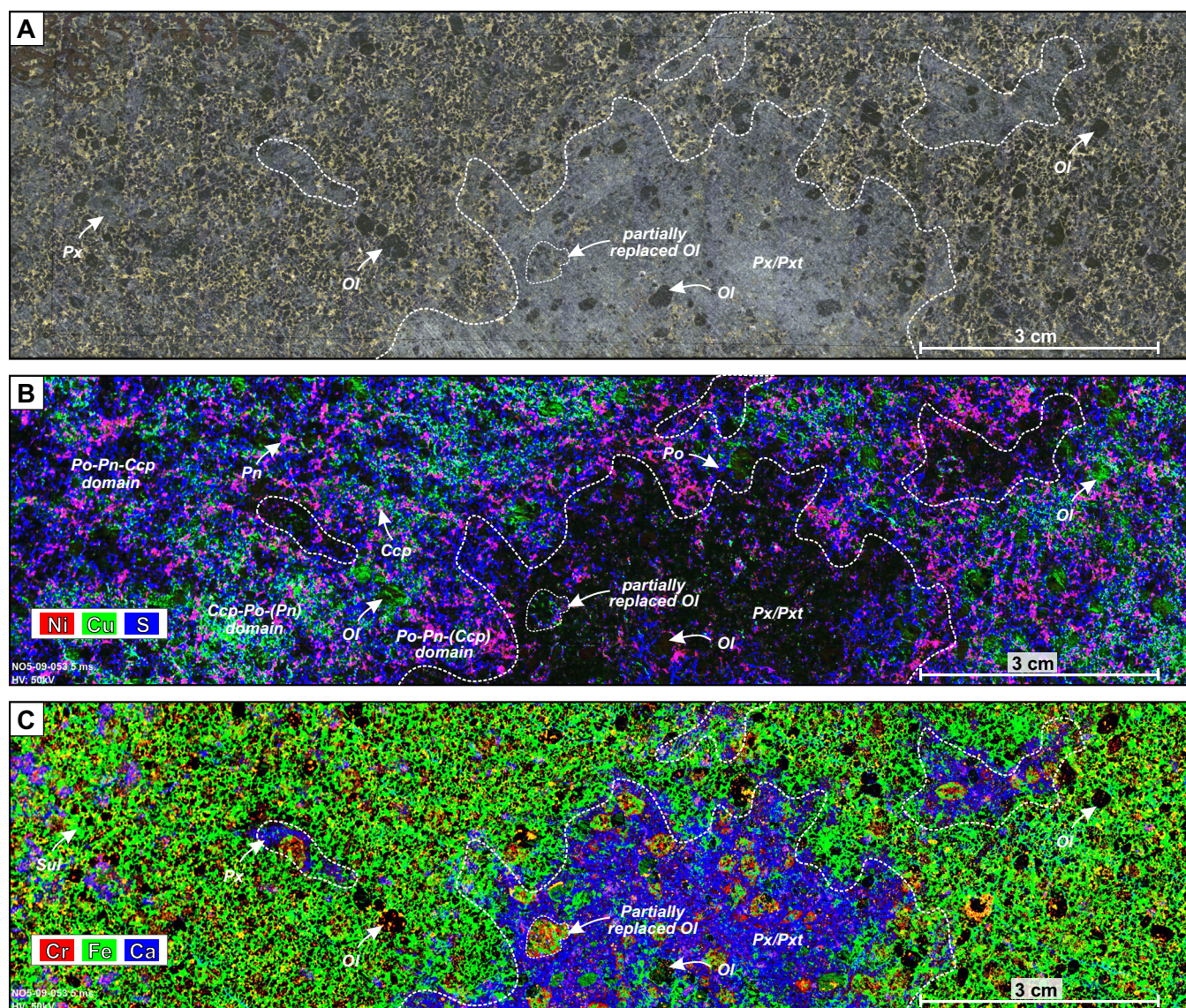


Figure 7. Disrupted net-textured sulphide subfacies from the Eagle's Nest deposit (drill core NOT-09-053 at 857.26 m, NQ core size). **a)** A scanned slab of typical disrupted net-textured sulphide. The black minerals are olivine and the yellowish minerals are sulphide. **b)** μ XRF map with normalized relative concentrations of Ni (red), Cu (green), and S (blue) showing three main sulphide domains (see text for discussion). **c)** μ XRF map with normalized relative concentrations of Cr (red), Fe (green), and Ca (blue). White dotted lines indicate the gradational contact between the pyroxenite and the net-textured sulphide facies into the disrupted net-textured sulphide subfacies rock. Abbreviations: Ccp = chalcopyrite, Ol = olivine, Pn = pentlandite, Po = pyrrhotite, Px = pyroxene, Pxt = pyroxenite.

in Figure 7. The optical image (Fig. 7a) indicates that sulphide is much more abundant in leopard net-textured domains containing abundant fine-grained serpentinized olivine (black) and much less abundant in areas where pyroxene (grey) occurs as pyroxenite. The Ni-Cu-S map (Fig. 7b), highlights three main sulphide domains that border the areas of pyroxenite, progressing outward from (1) pyrrhotite (blue) \approx pentlandite (magenta) \gg chalcopyrite (green) through (2) chalcopyrite \gg pyrrhotite \approx pentlandite to (3) pyrrhotite \approx pentlandite $>$ chalcopyrite. In the Cr-Fe-Ca map (Fig. 7c), the distinction between the pyroxenitic material (blue), which contain patches of residual olivine (black), ferrichromite (yellow), and chromite (red), and

the surrounding net-textured sulphides (green; all sulphide species), is more distinct.

Massive to Semi-massive Sulphide Facies

Massive sulphide facies at Eagle's Nest contains >80 wt% sulphides and >31 wt% S and is localized mainly in two embayments along the (original) basal contact (Fig. 2). Gangue phases include inclusions of peridotite and calcite. Semi-massive sulphide, which is very uncommon in the Eagle's Nest deposit, contains 50–80 wt% sulphides and ~ 20 –31 wt% S depending on the proportion of inclusions present. It occurs in the lower parts of the deposit in contact with country rocks (more common) and the upper parts of the deposit in contact

with barren ultramafic rocks (less common). The non-sulphide component is normally composed of gabbro or granodiorite xenoliths derived from the country rocks, and pyroxenite and peridotite anteliths or autoliths ("cognate xenoliths") derived from this or other phases of the intrusive system. Although much less common, sulphide-bearing inclusions also occur within this facies and are normally composed of leopard net-textured sulphides. Semi-massive sulphides contain no olivine and pyroxene crystals, except within ultramafic inclusions. The sulphides are similar to those found in the massive sulphide facies.

A contact between semi-massive and massive sulphide facies is shown in Figure 8 (optical scan in Fig. 8a, μ XRF maps in Fig. 8b,c). The amount of sulphide varies from ~60% in semi-massive sulphides (left side of image) to ~95% in massive sulphides (right side of image). The semi-massive sulphide domain contains abundant inclusions of altered, recrystallized, and partially melted gabbro. In the Ni-Cu-S map (Fig. 8b), it is clear that the semi-massive sulphides are composed of pyrrhotite (blue) >> pentlandite (magenta) chalcopyrite (cyan) and that the massive sulphides are composed of pyrrhotite > pentlandite chalcopyrite. Pentlandite and chalcopyrite are finer grained and more dispersed (occurring as patches and along pyrrhotite grain boundaries) in semi-massive sulphides, and coarser grained and more segregated in massive sulphides. In the Cr-Fe-Ca map (Fig. 8c), pyrrhotite is bright green, and pentlandite and chalcopyrite are both dark green. The sulphide minerals display a combination of coarse granular pentlandite (at contacts with chalcopyrite) and thin (sub-mm) "loops" of exsolved pentlandite (commonly in semi-massive sulphide around pyrrhotite grain boundaries, Fig. 8c). The inclusions contain a Ca-rich phase (dark blue), likely altered clinopyroxene based on the mineral habit, and a Cr-Fe-Ca-poor phase (black), likely altered (albitic) plagioclase. Ferrichromite (orange-yellow) occurs as isolated crystals and as rims on inclusions.

DISCUSSION

Maps obtained by μ XRF provide greatly enhanced textural, mineralogical, and geochemical characterizations compared that obtained from macroscopic core logging and microscopic petrographic examination. In particular, they provide detailed geochemical information that is not available by either of the other methods and at a scale larger than permitted by SEM-based ED-XRES, EPMA-based WD-XRES, or LA-ICP-MS methods¹.

Below we further discuss some of the textures in Eagle's Nest ores and their implications for the genesis of the mineralization.

Mineralogical Insights

Clinopyroxene and orthopyroxene in pinto and disrupted net-textured sulphide subfacies

Superimposed talc-carbonate alteration commonly hampers identifications of primary mineralogy, but μ XRF maps make it possible to readily distinguish between serpentine-magnetite pseudomorphs after olivine in leopard net-textured sulphide, talc±anthophyllite pseudomorphs after orthopyroxene and Ca-rich amphibole pseudomorphs after clinopyroxene in pinto net-textured sulphide, and Ca-pyroxene pseudomorphs after clinopyroxene in disrupted net-textured sulphide.

In pinto net-textured sulphides (Fig. 5), the μ XRF maps indicate that clinopyroxene occurs as evenly distributed, fine-grained (0.1–0.2 mm) subhedral crystals, whereas orthopyroxene occurs both as evenly distributed, medium-grained (0.3–10 mm) rounded crystals typically associated with clinopyroxene, and as coarse-grained (up to 15 mm) irregular aggregates. The composite orthopyroxene-clinopyroxene crystals are evenly distributed and appear to have nucleated more-or-less homogeneously, locally impinging on each other to form coarser aggregates. Both pyroxenes are devoid of sulphides, suggesting that they crystallized from the silicate melt prior to the introduction of sulphide liquid.

In disrupted net-textured (Fig. 7), the μ XRF maps indicate that the clinopyroxene has replaced smaller olivine crystals and possibly sulphide, leaving behind coarser olivine crystals and aggregates. The nature of this process is discussed further below.

Sulphide inclusions in olivine

The presence of pyrrhotite as uncommon blebs within olivine and pyroxene may represent (1) mobilization of sulphides into fractures in olivine after serpentinization (large fracture in olivine seen in Fig. 6), or (2) sulphidation of magnetite formed during serpentinization, as observed at the Raglan mine in Quebec (Bazilevskaya, 2009).

Monosulphide Solid Solution Segregation

Small-scale monosulphide solid solution segregation

The greater segregation of Cu and Fe-Ni in inclusion net-textured (Fig. 6), disrupted net-textured (Fig. 7), and massive (Fig. 8) sulphide textures is attributed to segregation of Cu-rich residual sulphide liquid from Fe-Ni-rich monosulphide solid solution (mss) (see review of phase equilibria by Naldrett, 2004). In the net-textured sulphide subfacies, the inclusions may have phys-

¹ ED = energy dispersive, EPMA = electron probe microanalyzer, LA-ICP-MS = laser ablation-inductively coupled plasma-mass spectrometry, SEM = scanning electron microscope, WD = wavelength-dispersive, XRES = X-ray emission spectrometry.

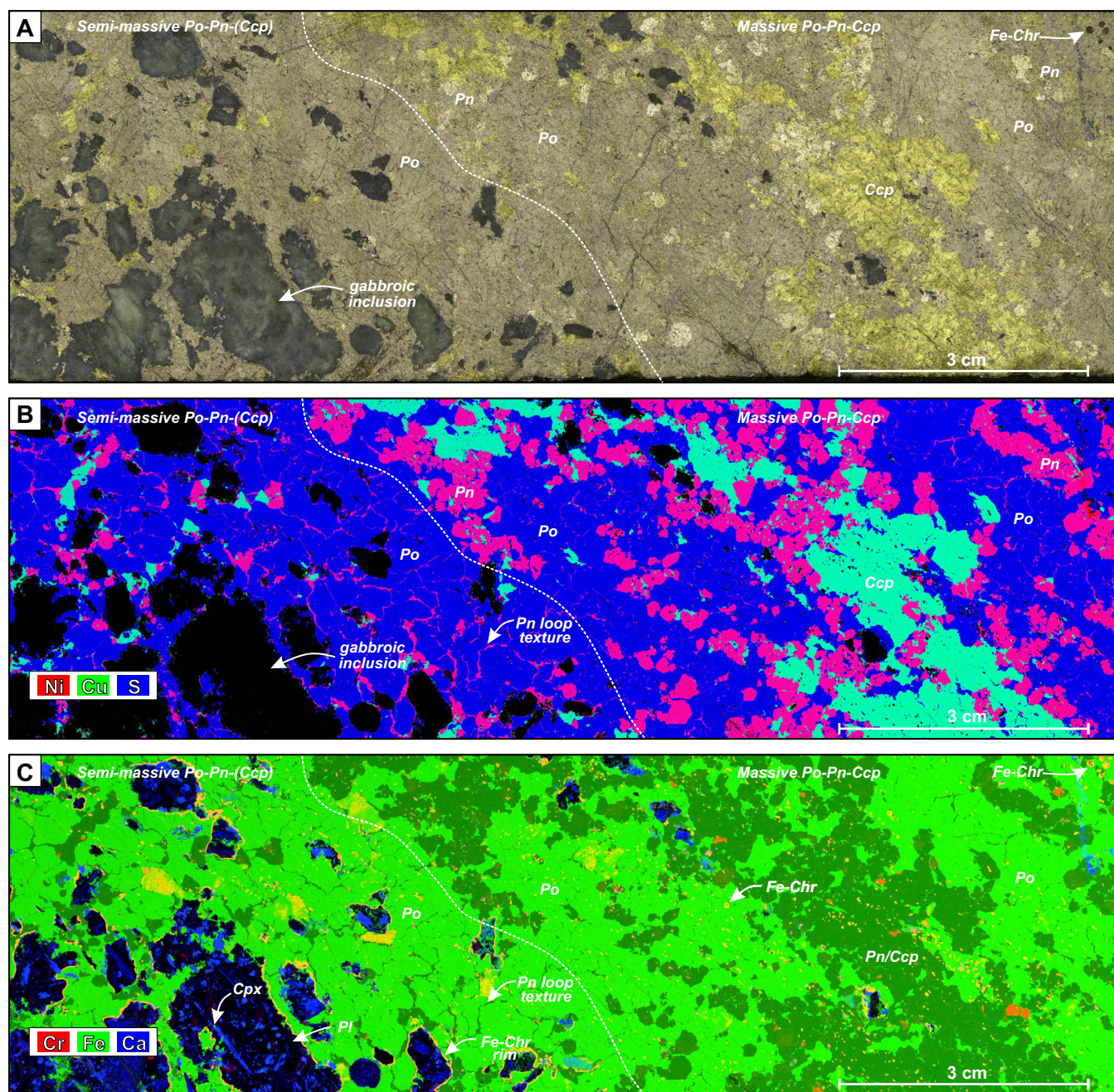


Figure 8. Massive and semi-massive sulphide facies at the Eagle's Nest deposit (drill core NOT-10-087A at 608 m, NQ core size). **a)** A scanned slab of typical semi-massive sulphides containing numerous gabbroic inclusions (dark grey on the left side) and massive sulphide (right side). The yellowish minerals are sulphide and fine black minerals are fine ferrichromite. **b)** μ XRF map with normalized relative concentrations of Ni (red), Cu (green), and S (blue). **c)** μ XRF map with normalized relative concentrations of Cr (red), Fe (green), and Ca (blue). The coarse yellow patches within the pyrrhotite crystals in this image are diffraction artifacts. Abbreviations: Ccp = chalcopyrite, Cpx = clinopyroxene, Fe-Chr = ferrichromite, Pl = plagioclase, Pn = pentlandite, Po = pyrrhotite.

ically facilitated migration of sulphide liquid from mss, and the emplacement of the late pyroxenite may have slowed cooling and/or reheated the mineralization.

Large-scale monosulphide solid solution-melt segregation

Pyrrhotite±pentlandite veinlets locally crosscut the fabrics of net-textured ores and locally also olivine and

pyroxene grains (Fig. 4, 6). They appear to be oriented at steep angles to the basal contact of the intrusion. The abundance of pyrrhotite-pentlandite and paucity of chalcopyrite in the veinlets suggests that they represent the lower temperature equivalents of higher temperature Fe-Ni-(Co)-rich mss. Two possible origins are (1) solid-state mobilization of mss into the veinlets during volume expansion accompanying serpentinization of

olivine (which we consider less likely based on the mineralogy, textures, and orientation), and (2) crystallization of mss from a sulphide liquid as it percolated downward through the crystal network of olivine crystals, from which the residual Cu-rich sulphide liquid escaped (which we consider more likely based on the same features). In the latter case, some of the Cu-rich sulphide liquid may have infiltrated other areas, forming complementary chalcopyrite-rich mineralization represented by sporadic chalcopyrite-rich veins (e.g. Fig. 2). Further study of relationships between the veinlets and serpentine-magnetite alteration should provide better insights into the relative roles of each process.

Multistage Silicate-Sulphide Emplacement

Country-rock inclusions

The presence of barren gabbro inclusions only in semi-massive sulphide (Fig. 8) indicates that only this phase of mineralization incorporated gabbroic country rocks prior to reaching this part of the system. The reason for the restriction to these facies is not known but would require a separate phase of emplacement. The thin, semi-continuous ferrichromite rims along the margins of the gabbro inclusions against sulphide suggest reaction with sulphide liquid. These rims are similar to ferrichromites that occur along the basal and upper margins of massive sulphides in other komatiite-associated Ni-Cu-(PGE) deposits (e.g. Kambalda: Groves et al., 1977; Silver Swan: Dowling et al., 2004; Alexo: Houlé et al., 2012; *see also* Fonseca et al., 2008). Gabbroic inclusions have significantly lower densities (~ 2.9 g cm $^{-3}$) than sulphide liquid (~ 4.2 g cm $^{-3}$), so unless connected in 3-D, all but the smallest inclusions would rapidly rise through sulphide liquid (*see* Leshner, 2017). If so, this means (1) they could not have been transported over significant distances, and (2) they must have been incorporated shortly before the sulphide liquid began to crystallize. Alternatively, the gabbroic inclusions could also represent sulphide-silicate emulsion textures, which also exhibit fine chromite rims (e.g. Frost and Groves, 1989; Staude et al., 2017). In this case, the “inclusions” might be connected in 3-D to the original contact (*see* Dowling et al., 2004). However, thus far, no evidence of such a connection has been observed to support this interpretation.

Anteliths

The presence of inclusions of barren peridotite only within disseminated and inclusion net-textured sulphides (Fig. 6) indicates that only these phases of mineralization incorporated anteliths “upstream” in the system or within this part of the system. The latter is more likely because the angular margins of some of the inclusions would likely not have survived during transport-related thermochemical sulphide erosion.

Chromitite and chromite-peridotite inclusions

The presence of ellipsoidal inclusions of chromitite (Fig. 3) and net-textured chromitite in disseminated sulphide (Fig. 3), but not in any of the other textural types, indicates that the disseminated sulphides formed from a different magma or that chromite xenoliths were completely assimilated in other textures. The chromite inclusions were coarser and denser (1–2 cm, ~ 5.2 g cm $^{-3}$) than associated olivine (3–5 mm, ~ 3.2 g cm $^{-3}$), so should have settled much more rapidly (*see* Leshner, 2017). This suggests that the magmas that formed the disseminated mineralization were emplaced after the magma that formed the underlying net-textured mineralization and that the chromite inclusions were transported from “upstream” of the plumbing system. The chromite inclusions may represent chromitite that crystallized in a staging chamber and was mechanically eroded, or the inclusions may represent refractory magnetite layers (e.g. massive chromitite inclusions) that were disrupted and upgraded to chromite during transport, similar to the process envisioned for the chromite horizons in the overlying Esker intrusive complex (Leshner et al., 2019).

Disrupted net-textured sulphide facies

One of the main characteristics of the disrupted net-textured sulphide facies is its very localized and heterogeneous distribution throughout the deposit (Zuccarelli et al., 2017, 2018b). This heterogeneity is well illustrated at the deposit scale in Figure 2, but also at the mesoscopic scale in Figure 7 where domains (2–5 cm) of barren pyroxenite are surrounded by more typical net-textured sulphide. Several scenarios have been evaluated by Zuccarelli (in prep) to explain disrupted net-textured sulphide: 1) early downward gravitational percolation of molten sulphide; 2) invasion by a late magmatic pyroxenitic melt, as proposed by Spath (2017) for the Black Label chromite zone of the Black Thor intrusion of the Esker intrusive complex a few kilometres to the northeast; 3) infiltration by a late magmatic Ca-Si-rich fluid, converting olivine to pyroxene, as proposed for the Ntaka ultramafic complex, Tanzania by Barnes et al. (2016); and/or 4) variable degrees of metamorphic alteration.

A detailed discussion of each hypothesis is beyond the scope of this contribution; however, μ XRF mapping (Fig. 7b,c) shows that some olivine has been transgressed by pyroxene rather than corroded by it. This favours physical invasion by a more fractionated magma that crystallized pyroxenite rather than the reaction of olivine with a Ca-Si-rich fluid to produce pyroxene, which is consistent with the occurrence of pyroxenite also crosscutting barren peridotite elsewhere within the Eagle's Nest intrusion (Zuccarelli, in prep) and in the nearby Black Label chromite zone (Spath, 2017).

The zonation of sulphides outward from pyroxenite in Figure 7b most likely reflects the partial melting of the Fe-Ni-Cu sulphides, mobilizing a Cu-rich sulphide melt and leaving behind a Cu-poor mss.

Late Sulphide Mobilization

The veins of massive pentlandite-pyrrhotite-chalcopyrite and chalcopyrite-pyrrhotite-pentlandite that cross-cut disseminated and net-textured facies could represent separate late injections of massive sulphide liquids from upstream in the conduit, but more likely represent late mobilization of a molten sulphide liquid within the conduit. Fe-Ni-Cu sulphides crystallize at temperatures of between 1160 and 850°C (*see* review of phase equilibria by Naldrett, 2004), which is below the 1360–1200°C temperature over which the host rocks would have crystallized (*see* review by Arndt et al., 2008).

CONCLUSIONS

The wide variety of sulphide textures within the Eagle's Nest orebody have been characterized using μ XRF, adding critical geochemical and mineralogical information that has greatly expanded and improved our understanding of the geological history and genesis of the ores.

The μ XRF scans more clearly define the textural differences between each sulphide facies and subfacies as well as other distinguishing features: 1) chromitite inclusions in disseminated sulphides, 2) mesocrysts and aggregates of serpentinized olivine in leopard net-textured sulphides, 3) altered orthopyroxene oikocrysts in pinto net-textured sulphides, 4) peridotite anteliths in inclusion net-textured sulphides, 5) transgressive pyroxenite in disrupted net-textured sulphides, 6) gabbro inclusions in semi-massive sulphides, and 7) small- and large-scale segregation of mss and residual sulphide liquids in many of these facies. Different types of inclusions in disseminated, inclusion net-textured, and semi-massive sulphides, and the presence of late pyroxenite suggest that the inclusions were emplaced in separate "pulses".

ACKNOWLEDGMENTS

This report is a contribution to NRCan's Targeted Geoscience Initiative Program (TGI). Support for this study was provided through the Orthomagmatic Ni-Cu-PGE-Cr Ore Systems Project's 'Activity NC-2.1: Architecture of magmatic conduits in Cr-(PGE)/Ni-Cu-(PGE) ore systems'.

Nataschia Zuccarelli is conducting a TGI-supported M.Sc. thesis at Laurentian University, Sudbury, Ontario. The authors are thankful to Noront Resources Ltd. (Alan Coutts, Ryan Weston, Matt Downey, and the Esker exploration team) for providing access to properties and geological information. We are also grateful to

Ryan Weston, Matt Deller, and Geoff Heggie from Noront Resources Ltd. for their strong support throughout the project, insightful discussions, and sharing of knowledge on the geology and mineralization of the Eagle's Nest deposit. The μ XRF mapping was carried out at the CSIRO characterization facility in Perth, Western Australia, and Michael Verrall is thanked for assistance and laboratory maintenance. This report benefited from scientific reviews by Charley Duran and Wouter Bleeker, and editorial review by Elizabeth Ambrose and Valérie Bécu.

REFERENCES

- Arndt, N., Leshner, C.M., and Barnes, S.J., 2008. Komatiite; Cambridge University Press, Cambridge, United Kingdom, 467 p. (first edition)
- Barnes, S.J. and Mungall, J.E., 2018. Blade-shaped dikes and nickel sulphide deposits: a model for the emplacement of ore-bearing small intrusions; *Economic Geology*, v. 113, p. 789–798.
- Barnes, S.J., Mole, D.R., Le Vaillant, M., Campbell, M.J., Verrall, M.R., Roberts, M.P., and Evans, N.J., 2016. Poikilitic textures, heteradcumulates and zoned orthopyroxenes in the Ntaka Ultramafic Complex, Tanzania: Implications for crystallization mechanisms of oikocrysts; *Journal of Petrology*, v. 57, p. 1171–1198.
- Barnes, S.J., Mungall, J.E., Le Vaillant, M.L., Godel, B., Leshner, C.M., Holwell, D.M., Lightfoot, P.C., Krivolutskaia, N., and Wei, B., 2017. Sulphide-silicate textures in magmatic Ni-Cu-PGE sulphide ore deposits: Disseminated and net-textured ores; *American Mineralogist*, v. 102, p. 473–506.
- Bazilevskaya, E., 2009. Primary and secondary textures of Fe-Ni-Cu sulfide mineralization in the Katinniq member of the Raglan Formation, Cape Smith Belt, New Quebec; M.Sc. thesis, Laurentian University, Sudbury, Ontario, 59 p.
- Dowling, S.E., Barnes, S.J., and Hill, R.E.T., 2004. Komatiites and nickel sulfide ores of the Black Swan area, Yilgarn Craton, Western Australia. 2: Geology and genesis of the orebodies; *Mineralium Deposita*, v. 39, p. 707–728.
- Frost, K.M. and Groves, D.I., 1989. Magmatic contacts between immiscible sulfide and komatiitic melts; implications for genesis of Kambalda sulfide ores; *Economic Geology*, v. 84, p. 1697–1704.
- Fonseca, R.O.C., Campbell, I.H., O'Neill, H.St.C., and Fitzgerald, J.D., 2008. Oxygen solubility and speciation in sulphide-rich mattes; *Geochimica et Cosmochimica Acta*, v. 72, p. 2619–2635.
- Groves, D.I., Barrett, F.M., Binns, R.A., and McQueen, K.G., 1977. Spinel phases associated with metamorphosed volcanic-type iron-nickel sulfide ores from Western Australia; *Economic Geology*, v. 72, p. 1224–1244.
- Houlé, M.G., Leshner, C.M., and Davis, P.C., 2012. Thermo-mechanical erosion at the Alexo mine, Abitibi greenstone belt, Ontario: Implications for genesis of komatiite-associated Ni-Cu-(PGE) mineralization; *Mineralium Deposita*, v. 47, p. 105–128.
- Houlé, M.G., Leshner, C.M., Metsaranta, R.T., and Sappin, A.-A., 2019. Architecture of magmatic conduits in chromium-PGE and Ni-Cu-PGE ore systems in Superior Province: Example from the 'Ring of Fire' region, Ontario; *in* Targeted Geoscience Initiative: 2018 report of activities, (ed.) N. Rogers; Geological Survey of Canada, Open File 8549, p. 441–448.
- Houlé, M.G., Leshner, C.M., Metsaranta, R.T., Sappin, A.-A., Carson, H.E.J., Schetselaar, E., McNicoll, V., and Laudadio, A., 2020. Magmatic architecture of the Esker intrusive complex,

- Ring of Fire intrusive suite, McFaulds Lake greenstone belt, Superior Province, Ontario: Implications for the genesis of Cr and Ni-Cu-(PGE) mineralization in an inflationary dyke-chonolith-sill complex; *in* Targeted Geoscience Initiative 5: Advances in the understanding of Canadian Ni-Cu-PGE and Cr ore systems – Examples from the Midcontinent Rift, the Circum-Superior Belt, the Archean Superior Province, and Cordilleran Alaskan-type intrusions, (ed.) W. Bleeker and M.G. Houlé; Geological Survey of Canada, Open File 8722, p. 141–163.
- Laudadio, A., 2019. 3D Geological Modeling of the Double Eagle–Black Thor Intrusive Complexes, McFaulds Lake Greenstone Belt, Ontario, Canada; M.Sc. thesis, Carleton University, Ottawa, Ontario, 107 p.
- Leshner, C.M., 2017. Roles of residues/skarns, xenoliths, xenocrysts, xenomelts, and xenovolatiles in the genesis, transport, and localization of magmatic Fe-Ni-Cu-PGE sulfides and chromite; *Ore Geology Reviews*, v. 90, p. 465–484.
- Leshner, C.M., Carson, H.J.E., and Houlé, M.G., 2019. Genesis of chromite deposits by dynamic upgrading of Fe±Ti oxide xenocrysts; *Geology*, v. 47, p. 207–210.
- Metsaranta, R.T., Houlé, M.G., McNicoll, V.J., and Kamo, S.L., 2015. Revised geological framework for the McFaulds Lake greenstone belt, Ontario; *in* Targeted Geoscience Initiative 4: Canadian Nickel-Copper-Platinum Group Elements-Chromium Ore Systems — Fertility, Pathfinders, New and Revised Models, (ed.) D.E. Ames and M.G. Houlé; Geological Survey of Canada, Open File 7856, p. 61–73.
- Mungall, J.E., Harvey, J.D., Balch, S.J., Azar, B., Atkinson, J., and Hamilton, M.A., 2010. Eagle's Nest: A Magmatic Ni-Sulfide Deposit in the James Bay Lowlands, Ontario, Canada; Chapter 28 *in* The Challenge of Finding New Mineral Resources: Global Metallogeny, Innovative Exploration, and New Discoveries, (ed.) R.J. Goldfarb, E.E. Marsh, and T. Monecke; Society of Economic Geologists, Special Publication 15, v. 1, p. 539–557.
- Naldrett, A.J., 2004. Magmatic Sulfide Deposits: Geology, Geochemistry and Exploration; Springer, Berlin, Germany, New York, New York, 727 p. (first edition)
- Spath, C.S., III, 2017. Geology and Genesis of Hybridized Ultramafic Rocks in the Black Label Hybrid Zone of the Black Thor Intrusive Complex, McFaulds Lake Greenstone Belt, Ontario, Canada; M.Sc. thesis, Laurentian University, Sudbury, Ontario, 94 p.
- Staude, S., Barnes, S.J., and Le Vaillant, M., 2017. Thermo-mechanical excavation of ore-hosting embayments beneath komatiite lava channels: textural evidence from the Moran deposit, Kambalda, Western Australia; *Ore Geology Review*, v. 90, p. 446–464.
- Zuccarelli, N., in prep. Textural sulphide facies at Eagle's Nest Ni-Cu-(PGE) deposit; M.Sc. thesis, Laurentian University, Sudbury, Ontario.
- Zuccarelli, N., Leshner, C.M., Houlé, M.G., and Weston, R.J., 2017. Sulfide textural variations and multiphase ore emplacement in the Eagle's Nest Ni-Cu-PGE deposit, McFaulds Lake greenstone belt, Ontario, Canada; Society for Geology Applied to Mineral Deposits, Proceedings of the 14th SGA Biennial Meeting, p. 583–586.
- Zuccarelli, N., Leshner, C.M., Houlé, M.G., and Weston, R.J., 2018a. Sulfide textural variations and multiphase ore emplacement in the Eagle's Nest Ni-Cu-(PGE) deposit, McFaulds Lake greenstone belt, Superior Province, northern Ontario, Canada; Geological Society of America, Abstracts with Programs, v. 50. doi:10.1130/abs/2018AM-317024
- Zuccarelli, N., Leshner, C.M., and Houlé, M.G., 2018b. Sulphide textural variations and multiphase ore emplacement in the Eagle's Nest Ni-Cu-(PGE) deposit, McFaulds Lake greenstone belt, Ontario; *in* Targeted Geoscience Initiative: 2017 report of activities, volume 2, (ed.) N. Rogers; Geological Survey of Canada, Open File 8373, p. 29–34.

